

Optical matrix elements in Three-bands Tight binding model for Monolayer Transition Metal Dichalcogenides

Presenter

Dao Duy Tung ¹

Supervisor

Dr. Huynh Thanh Duc ²

¹University of Science, Ho Chi Minh city

²Institute of Applied Mechanics and Informatics, VAST

June 12, 2025

Outline

1 Overview

- Monolayer transition metal dichalcogenide systems

2 Electronic band structure

- Density functional theory
- Three-band tight-binding theory
- $\mathbf{k} \cdot \mathbf{p}$ theory

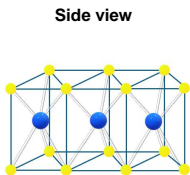
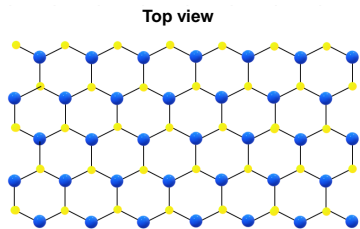
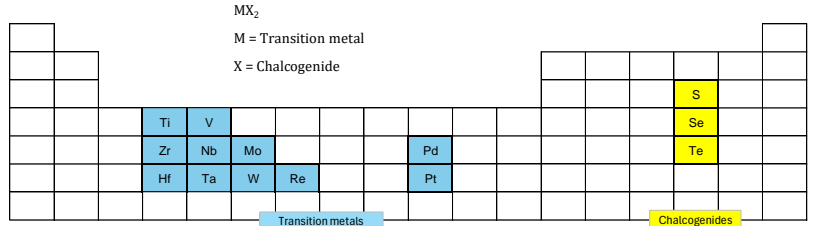
3 Optical selection rules

- Optical interband transitions

4 Summary and Outlook

- Main findings
- Future directions

Transition metal dichalcogenide monolayers



Reciprocal lattice
and 1st Brillouin zone

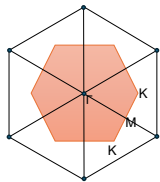


Figure: Transition metal dichalcogenides: elemental composition, atomic structure (top/side view), and 1st Brillouin zone

Transition metal dichalcogenide monolayers

Transition metal dichalcogenide (TMD) monolayers are semiconductors with a direct band gap

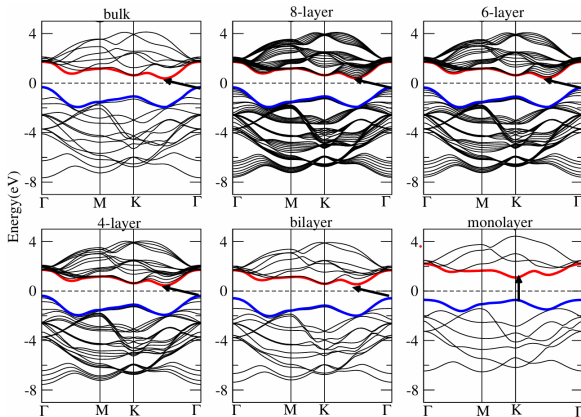
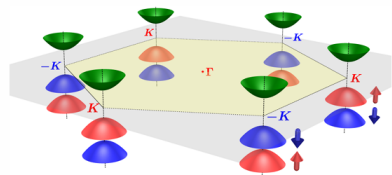


Figure: Electronic band structure of bulk MoS₂, its mono, and multilayers.¹

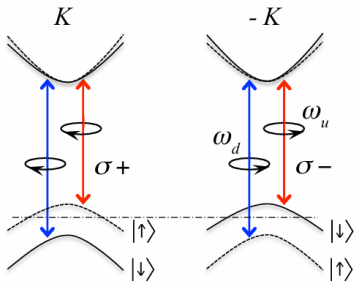
¹Kumar and Ahluwalia, "Electronic structure of TMDCs".

Transition metal dichalcogenide monolayers

TMD monolayers have a large spin splitting at band valleys



Schematic drawing of the band structure at the band edges



Valley and spin optical transition selection rules

Inversion asymmetry together with strong spin-orbit coupling (SOC) leads to a spin splitting of hundreds meV at the band valleys
⇒ Coupled spin and valley physics.²

²Xiao et al., "Coupled Spin and Valley Physics in Monolayers of MoS₂ and Other Group-VI Dichalcogenides".

Quantum ESPRESSO and Wannier90 software

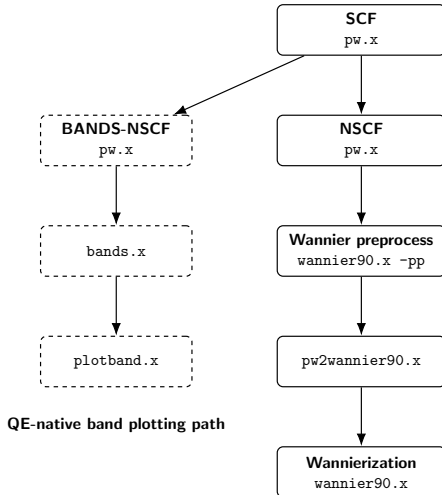


Figure: Workflow of WANNIER90 interfacing with QUANTUM ESPRESSO, including both the Wannierization path and the standard band structure plotting path.

Quantum ESPRESSO and Wannier90 software

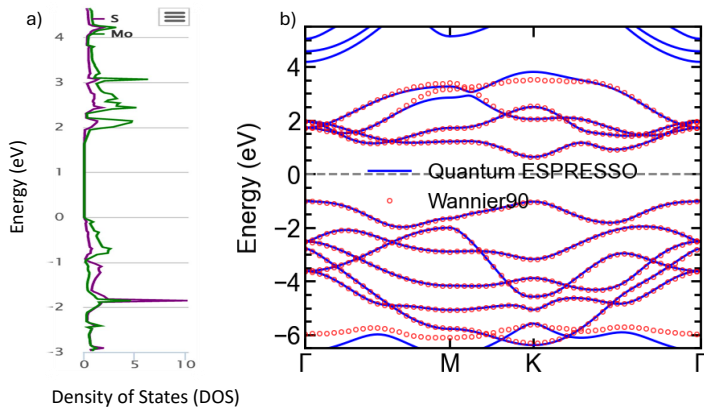


Figure: (a) Atom-projected density of states (DOS) for monolayer MoS₂³. (b) Band structure comparison between Quantum ESPRESSO (blue lines) and Wannier90 (red dots).

³ Materials Project.

Three-band tight-binding model

In this model, the basis consists of three d -orbitals of the M atom (neglecting the two S atoms near the band edges):

$$|d_{z^2}\rangle, \quad |d_{xy}\rangle, \quad |d_{x^2-y^2}\rangle$$

$$\psi_{\mathbf{k}}^{\lambda}(\mathbf{r}) = \sum_j C_{\mathbf{k}}^{\lambda}(j) \sum_{\mathbf{R}} e^{i\mathbf{k}\cdot\mathbf{R}} \phi_j(\mathbf{r} - \mathbf{R})$$

$$\sum_{j'} [H_{jj'}^{\text{TB}}(\mathbf{k}) - E_{\mathbf{k}}^{\lambda} S_{jj'}(\mathbf{k})] C_{\mathbf{k}}^{\lambda}(j) = 0$$

$$H_{jj'}^{\text{TB}} = \sum_{\mathbf{R}} e^{i\mathbf{k}\cdot\mathbf{R}} \langle \phi_j(\mathbf{r}) | \left[-\frac{\hbar^2 \nabla^2}{2m} + V \right] | \phi_{j'}(\mathbf{r} - \mathbf{R}) \rangle$$

The nearest-neighbor tight-binding (NN TB) Hamiltonian is showed as⁴

$$H^{\text{NN}}(\mathbf{k}) = \begin{bmatrix} h_0 & h_1 & h_2 \\ h_1^* & h_{11} & h_{12} \\ h_2^* & h_{12}^* & h_{22} \end{bmatrix}$$

⁴Liu et al., "Three-band tight-binding model for monolayers of group-VIB transition metal dichalcogenides".

Three-band tight-binding model

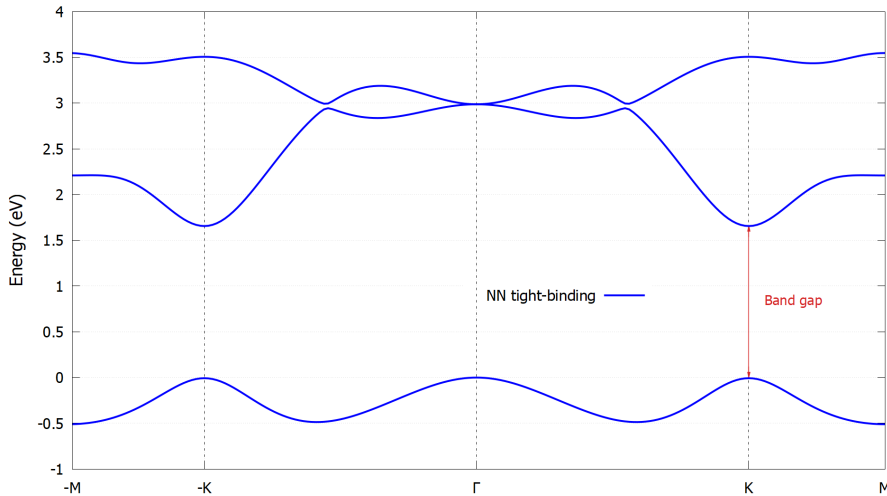


Figure: Bandstructure of monolayer MoS₂

$\mathbf{k}\cdot\mathbf{p}$ model

By using Löwdin partitioning method⁵, we can reduce the TBM basis to a two-band $\mathbf{k}\cdot\mathbf{p}$ model:

$$|\psi_c^\tau\rangle = |d_{z^2}\rangle, \quad |\psi_v^\tau\rangle = \frac{1}{\sqrt{2}} (|d_{x^2-y^2}\rangle + i\tau |d_{xy}\rangle)$$

where $\tau = \pm$ is the valley index

$$\psi_{\mathbf{k}}^\lambda(\mathbf{r}) = e^{i\mathbf{k}\cdot\mathbf{r}} \sum_j C_{\mathbf{k}}^\lambda(j) u_j(\mathbf{r})$$

$$\sum_{j'} [H_{jj'}^{\mathbf{k}\cdot\mathbf{p}}(\mathbf{k}) - E_{\mathbf{k}}^\lambda \delta_{jj'}] C_{\mathbf{k}}^\lambda(j') = 0$$

$$H_{jj'}^{\mathbf{k}\cdot\mathbf{p}}(\mathbf{k}) = \langle u_j \left[\left[-\frac{\hbar^2 \nabla^2}{2m} + V \right] u_{j'} \right] \rangle + \frac{\hbar^2 k^2}{2m} \delta_{jj'} + \frac{\hbar}{m} \mathbf{k} \cdot \langle u_j | (-i\hbar \nabla) | u_{j'} \rangle$$

⁵Löwdin, "A Note on the Quantum-Mechanical Perturbation Theory".

$k \cdot p$ model

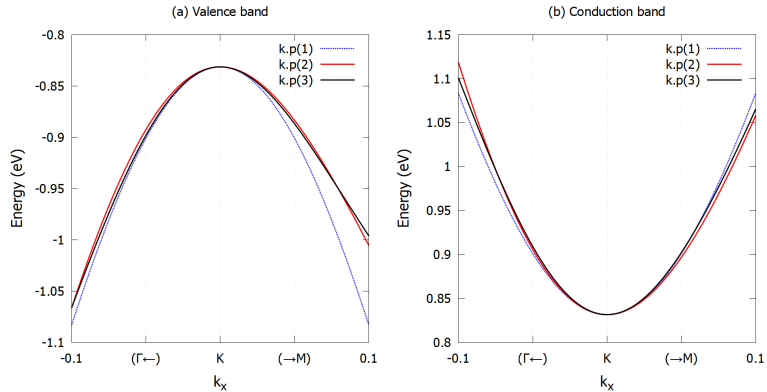


Figure: (a) Valence and (b) Conduction bands in the K valley of monolayer MoS₂ of $H_{kp}^{(1)}$, $H_{kp}^{(2)}$, $H_{kp}^{(3)}$, respectively.⁶

⁶Liu et al., "Three-band tight-binding model for monolayers of group-VIB transition metal dichalcogenides".

Bandstructures in three models

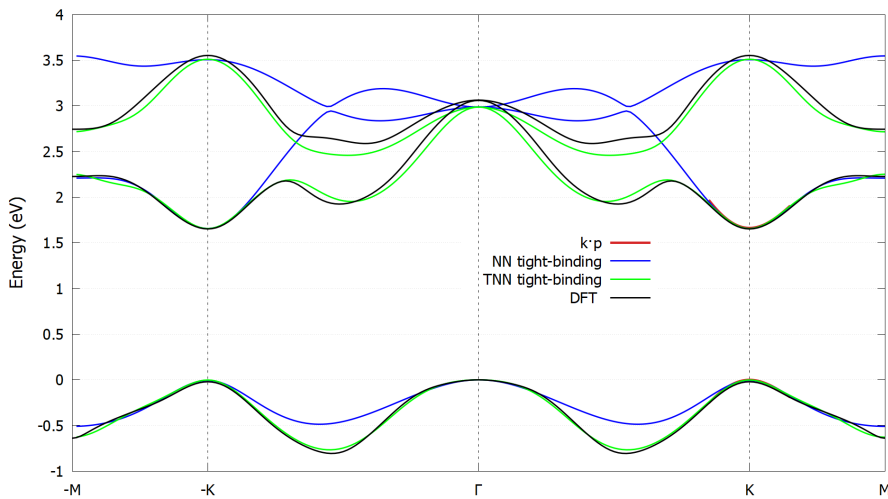


Figure: Comparison of MoS₂ bandstructures obtained from $k \cdot p$, nearest-neighbor TB, third-nearest-neighbor TB, and DFT models.

Optical interband transitions

The coupling strength with optical fields of σ_{\pm} circular polarization is given by

$$p_{\pm}(\mathbf{k}) \equiv p_x(\mathbf{k}) \pm i p_y(\mathbf{k})$$

where $p_{\alpha}(\mathbf{k}) \equiv m_0 \langle u_c(\mathbf{k}) | \frac{1}{\hbar} \frac{\partial \hat{H}}{\partial k_{\alpha}} | u_v(\mathbf{k}) \rangle$ is the interband matrix element of the canonical momentum operator and m_0 is the free electron mass.

In tight-binding model,

$$\begin{aligned} \langle \psi_{\lambda, \mathbf{k}} | \mathbf{p} | \psi_{\lambda', \mathbf{k}} \rangle &= \frac{m}{\hbar} \sum_{jj'} C_j^{\lambda*}(\mathbf{k}) C_{j'}^{\lambda'}(\mathbf{k}) \nabla_{\mathbf{k}} H_{jj'}(\mathbf{k}) \\ &\quad + i \frac{m}{\hbar} \sum_{jj'} C_j^{\lambda*}(\mathbf{k}) C_{j'}^{\lambda'}(\mathbf{k}) (\epsilon_{\lambda}(\mathbf{k}) - \epsilon_{\lambda'}(\mathbf{k})) \mathbf{d}_{jj'}, \end{aligned}$$

In $\mathbf{k} \cdot \mathbf{p}$ model,

$$\langle \psi_{\lambda \mathbf{k}} | \mathbf{p} | \psi_{\lambda' \mathbf{k}'} \rangle = \frac{m}{\hbar} \sum_{jj'} C_{\mathbf{k}}^{\lambda}(j) C_{\mathbf{k}}^{\lambda'}(j') \nabla_{\mathbf{k}} H_{jj'}^{\mathbf{k} \cdot \mathbf{p}}(\mathbf{k}),$$

Optical interband transitions

In DFT model⁷,

$$\langle \mathbf{k}n | \mathbf{p} | \mathbf{k}m \rangle = \frac{m_e}{\hbar} \sum_{NM} C_N^{\mathbf{k}n*} C_M^{\mathbf{k}m} \frac{\partial H_{NM}(\mathbf{k})}{\partial \mathbf{k}} + i \frac{m_e}{\hbar} (\epsilon_{\mathbf{k}n} - \epsilon_{\mathbf{k}m}) \sum_{NM} C_N^{\mathbf{k}n*} C_M^{\mathbf{k}m} \sum_{\mathbf{R}} \langle 0N | \mathbf{r} | \mathbf{R}M \rangle e^{i\mathbf{k}\cdot\mathbf{R}}.$$

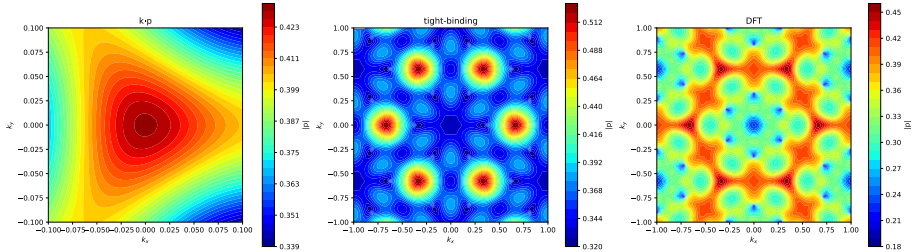


Figure: The absolute value of momentum $|p|^{cv} = \sqrt{|p_x|^2 + |p_y|^2}$ as a function of \mathbf{k} .

⁷Lee et al., "Tight-binding calculations of optical matrix elements for conductivity using nonorthogonal atomic orbitals: Anomalous Hall conductivity in bcc Fe".

Optical interband transitions

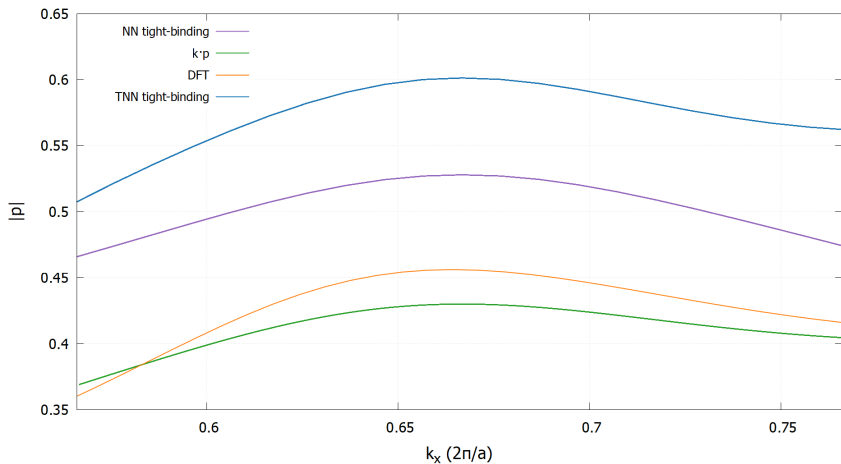


Figure: Comparison between DFT, nearest-neighbor TB (NN TB), third-nearest-neighbor TB (TNN TB) and $\mathbf{k} \cdot \mathbf{p}$ momentum dispersion curves in the vicinity of K valley.

Optical interband transitions

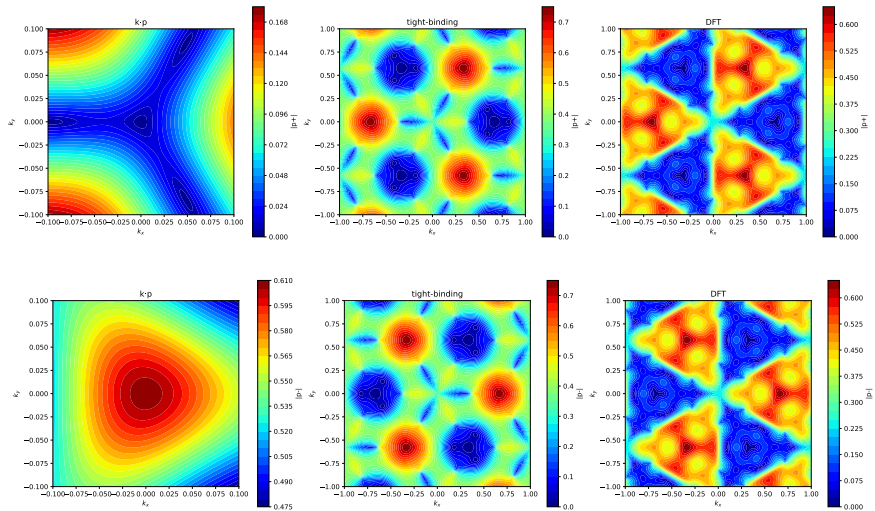


Figure: The absolute value of momentum p_+^{cv} and p_-^{cv} as a function of \mathbf{k} .

Main findings

Summary:

- Optical matrix elements of monolayer MoS₂ studied using tight-binding, $\mathbf{k}\cdot\mathbf{p}$, and DFT.
- Standard three-band TB model lacks accuracy in capturing intra-atomic effects with the used atomic orbitals.
- $\mathbf{k}\cdot\mathbf{p}$ model shows large deviations beyond the K valley.
- Both tight-binding and $\mathbf{k}\cdot\mathbf{p}$ models have limitations when compared to DFT.

Further research:

- Extend tight-binding models with more atomic orbitals for intra-atomic effects.
- Refine $\mathbf{k} \cdot \mathbf{p}$ model with higher-order terms and remote-band coupling.
- Study effects of strain, defects, and external fields on optical transitions, by applying the weak magnetic field.
- Solve the SBE using Wannier-interpolated band structure, dipole matrix elements, and Berry curvature obtained from QE and W90.

References

-  Kumar, A. and P. K. Ahluwalia. "Electronic structure of transition metal dichalcogenides monolayers 1H-MX₂ (M = Mo, W; X = S, Se, Te) from ab-initio theory: new direct band gap semiconductors". In: *European Physical Journal B* 85.6, 186 (June 2012), p. 186. DOI: 10.1140/epjb/e2012-30070-x.
-  Lee, Chi-Cheng et al. "Tight-binding calculations of optical matrix elements for conductivity using nonorthogonal atomic orbitals: Anomalous Hall conductivity in bcc Fe". In: *Phys. Rev. B* 98 (11 Sept. 2018), p. 115115. DOI: 10.1103/PhysRevB.98.115115. URL: <https://link.aps.org/doi/10.1103/PhysRevB.98.115115>.
-  Liu, Gui-Bin et al. "Three-band tight-binding model for monolayers of group-VIB transition metal dichalcogenides". In: *Phys. Rev. B* 88 (8 Aug. 2013), p. 085433. DOI: 10.1103/PhysRevB.88.085433. URL: <https://link.aps.org/doi/10.1103/PhysRevB.88.085433>.

References

-  Löwdin, Per-Olov. "A Note on the Quantum-Mechanical Perturbation Theory". In: *The Journal of Chemical Physics* 19.11 (Nov. 1951), pp. 1396–1401. ISSN: 0021-9606. DOI: 10.1063/1.1748067. eprint: https://pubs.aip.org/aip/jcp/article-pdf/19/11/1396/18799442/1396_1_online.pdf. URL: <https://doi.org/10.1063/1.1748067>.
-  Materials Project. URL: <http://www.materialsproject.org>.
-  Xiao, Di et al. "Coupled Spin and Valley Physics in Monolayers of MoS₂ and Other Group-VI Dichalcogenides". In: *Phys. Rev. Lett.* 108 (19 May 2012), p. 196802. DOI: 10.1103/PhysRevLett.108.196802. URL: <https://link.aps.org/doi/10.1103/PhysRevLett.108.196802>.